KnE Engineering

Knowledge E
Engaging minds

Conference Paper

Lead Sulfide Quantum Dot Sensitized Nanocrystalline Solar Cell

Khalil Ebrahim Jasim

Department of Physics, College of Science, University of Bahrain, P. O. Box 32038, Bahrain

Abstract

Solar cells were fabricated using lead sulfide (PbS) quantum dots (QDs) to sensitized nanocrystalline TiO_2 layer. The nanostructured layer of the TiO_2 was examined by scanning electron microscopy and X-ray diffraction spectroscopy. The data confirm the formation of nanostructured particles of sizes less than 50 nm. PbS quantum dots of three different sizes were used as sensitizers, and their absorption spectra were determined in order to characterize the optical properties of the cells. Current injection mechanisms and confinement effect on the electronic and optical properties of the cells were discussed. A model was developed to highlight the structure and operation of the cell. The I–V characteristics were measured either for specific size or mixed sizes of quantum dots. Power conversion efficiencies of up to 4.47% were obtained for cells using QDs of 3.2 nm radius as sensitizers.

Corresponding Author:
Khalil Ebrahim Jasim
khalilej@gmail.com

OPEN ACCESS

1. Introduction

For many decades, amorphous silicon and its alloys were among the best candidates of low cost solar cells [1-3]. Since the pioneering work of Grätzel in 1991 in developing dye synthesized solar cells, photoelectrochemical photovoltaic cells became the subject of intensive research work with promising solar efficiencies and reduced cost. These cells consist of a photoelectrode, a redox, an electrolyte, and a counter electrode [4]. A variety of dyes were used as sensitizers that absorb visible light. The excited electrons are then injected in the conduction band of a high gap semiconductor [5-10]. ZnO electrode sensitized by organic dyes including rose Bengal fluorescein and rhodamine, was first studied by Gerischer and Tributsch [11-12]. The realization of high performance nanoporous TiO_2 thin film electrodes announced a new era in the development of efficient synthesized solar cells. Photosensitizers such as Ru bipyridyl complexes were shown to be capable of absorbing radiation covering a wide range of the solar spectrum. Solar energy efficiencies of 11% under AM1.5 irradiation using

nanocrystalline TiO_2 thin film electrode have been reported [13]. Other materials such as ZnO_2 nanowires were proposed to replace both porous and TiO_2 nanoparticles-based solar cells [14]. The idea of injection of electrons in a wide bandgap semiconductor using a photosyntisizer is a key concept in developing photoelectrochemical photo-voltaic cells [15]. We investigate in this work the use of PbS quantum dots (QD) as a source of electron injection in TiO_2 porous thin film. Quantum dots are nanocrystals exhibiting a high degree of confinement, and extremely sharp density of state function. They have the outstanding property that their energy gap, and consequently their absorption threshold, depends on their sizes [16-18]. By choosing the right size of the QD, we can monitor the electron injection in the conduction band of the TiO_2 thin film. Furthermore, the possibility of creating multiple exciton by a single high energy photon has also revived the interest in these materials [19-20]. In this work we replace the natural dye extracts we reported [21-22] with QDs of different sizes as a source of electron injection.

Recently, many research works on QD synthesized solar cells have been published. The bulk of this work focuses on CdS, CdSe, and CdTe QD as synthesizers [23-25]. The choice of these materials follows the success of earlier studies on identifying the morphological and electrolyte effects on their performance and stability [26-27]. Inter-esting results have been reported by some investigators who studied the incorporation of a layer of PbS quantum dots in thin film solar cells, by direct growth of PbS quantum dots on nanostructured TiO_2 electrodes [28]. Deposition of a transition metal oxide (n-type) layer on grown layer of PbS quantum dots to act as hole extractor layers [29], or employing a graded recombination layer [30].

In this work we used colloidal PbS quantum dots as sensitizers for nanostructured TiO_2 layer, and demonstrate the effect of their sizes and other design parameters on the cell performance. The configuration and adherence of QDs to the TiO_2 nanostruc-tured thin film is illustrated schematically in Figure (1). In our approach to optimize the cell performance, we compare the efficiency obtained for the present system with that published elsewhere using similar QD synthesized based systems.

In the first part of this work we describe the preparation of nanostructured TiO_2 layer, followed by the process of QD application to its surface. In the second part we describe the photovoltaic cell preparation using various sizes of PbS quantum dots. In the last part we examine the structural, optical, electrical, and photovoltaic properties of the PbS QD sensitized photovoltaic cells.
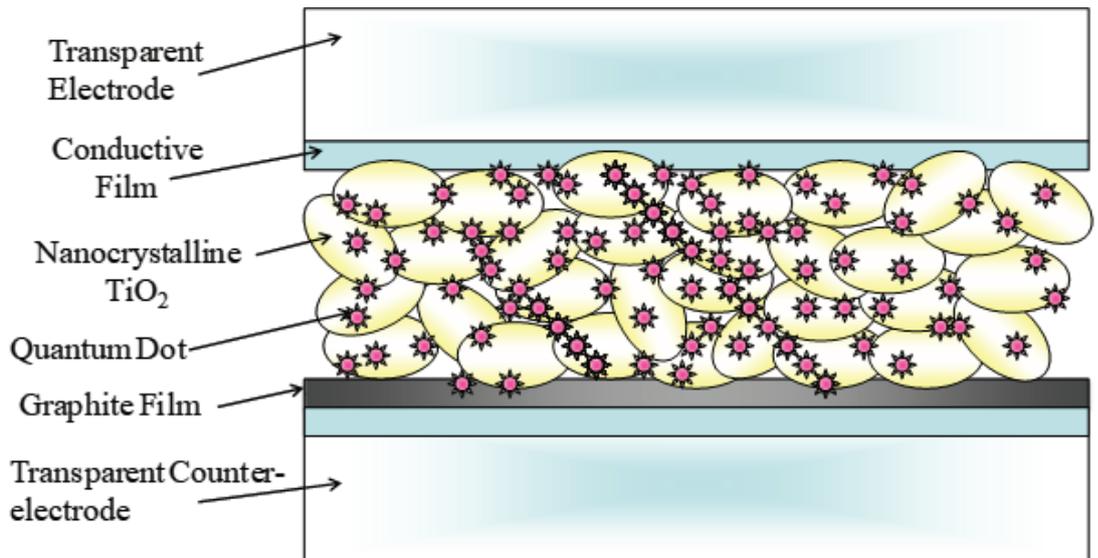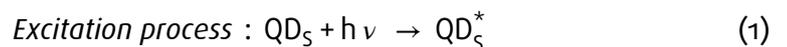
Figure 1: Schematic representation of the random distribution of QDs adhered to the TiO_2 nanocrystalline film.

2. Structure and Operation of QD Sensitized Photovoltaic Cell

The structure and operation principle of QD sensitized photovoltaic cell is almost identical to dye sensitized cells [31] with the exception that now the QDs are the source of current injection. The structure of the photovoltaic cell is shown schematically in Figure (2). In this figure, we distinguish four essential elements of the cell, namely, the conducting and counter conducting electrodes, the nanostructured TiO_2 layer, the quantum dot energy levels, and the electrolyte.
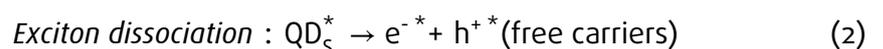
The operation of the cell can be described by the following steps and the corresponding process equations:

1. Upon absorption of a photon, a quantum dot is excited from the ground state (QD_S) to a higher energy state (QD_S^*), as illustrated by Eq.(1) below.

$$Excitation\ process : QD_S + h\nu \rightarrow QD_S^*$$ (1)

Where QD_S and QD_S^* is the quantum dot in its ground state and excited state respectively.

2. The absorption process results in the creation of electron-hole pair in the form of exciton. Dissociation of the exciton occurs if the thermal energy exceeds its binding energy.
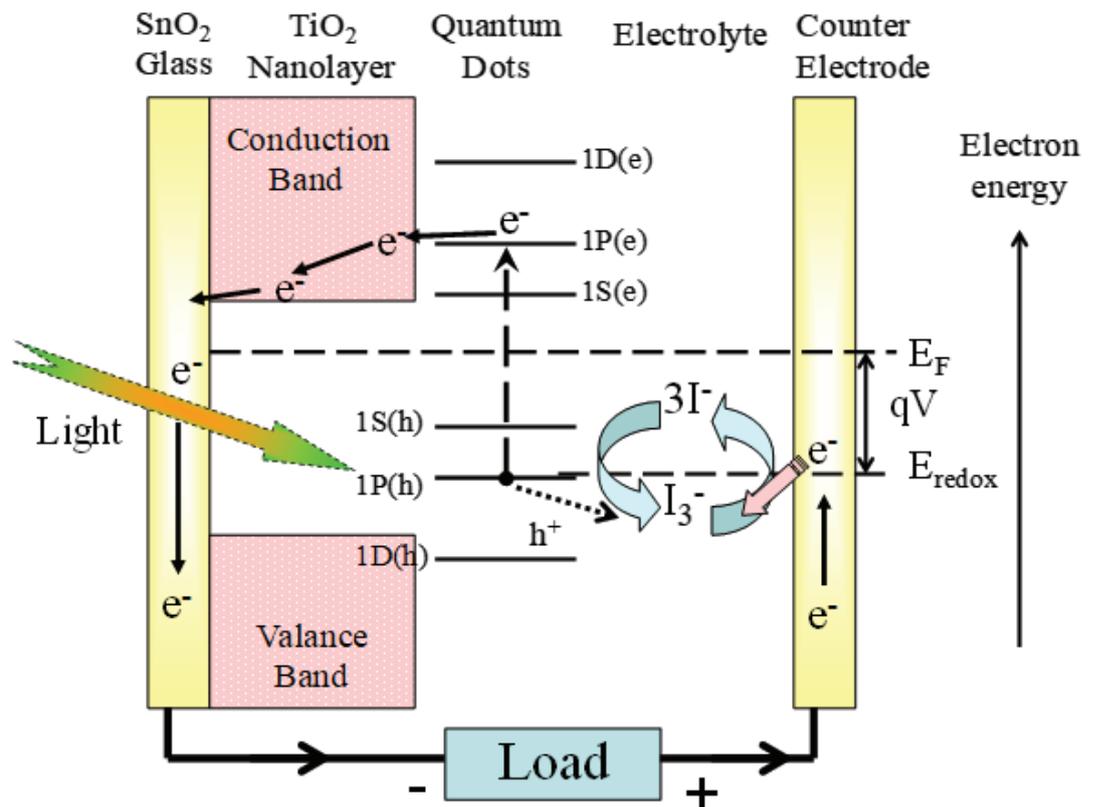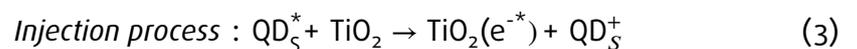
$$Exciton\ dissociation : QD_S^* \rightarrow e^{-*} + h^{+*} (free\ carriers)$$ (2)

Figure 2: Schematic diagram illustrating the structure and operation of quantum dots-synthesized solar cell.

3. The excited electron is then injected in the conduction band of the wide bandgap semiconductor nanostructured TiO_2 thin film. This process will cause the oxidation of the photosensitizer (The QDs).

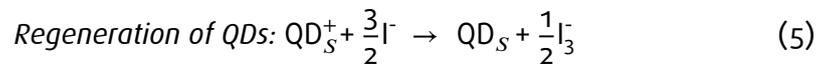$$Injection\ process : QD_S^* + TiO_2 \rightarrow TiO_2(e^{-*}) + QD_S^+ \tag{3}$$

4. The injected electron is transported between the TiO_2 nanoparticles, and then gets extracted to a load where the work done is delivered as electrical energy.

$$Energy\ generation: TiO_2(e^{-*}) + C.E. \rightarrow TiO_2 + e^{-*}(C.E.) + elecrical\ energy \tag{4}$$

Where C.E. stands for counter electrode. The counter electrode is identical to the photoelectrode where the nanostructured TiO_2 is deposited. The counter electrode is usually coated with a catalyst (graphite).

5. The electrolyte used in the cell contains I^-/I_3^- redox ions, that play the role of electron mediator between the TiO_2 photoelectrode and the counter electrode. Therefore, the oxidized photosensitizer states (QD_S^+) are regenerated by receiving

an electron from the oxidized I⁻ ion redox mediator, regenerating the ground state (QD$_S$), and I⁻ becomes oxidized to the oxidized state I$_3$⁻ (triodide ions).

$$\textit{Regeneration of QDs: } QD_S^+ + \frac{3}{2}I^- \rightarrow QD_S + \frac{1}{2}I_3^- \qquad (5)$$

6. The I$_3$⁻ diffuses to the counter electrode and substitutes the internally donated electron with that from the external load and gets reduced back to I⁻ ion.

$$\textit{Electron capture reaction: } \frac{1}{2}I_3^- + e^- (C.E) \rightarrow \frac{3}{2}I^- + C.E. \qquad (6)$$

Overall, generation of electric power in this type of cells causes no permanent chemical transformation.

To enhance electron injection into the conduction band of the TiO$_2$ layer, one must choose a sensitizer with a proper matching energy gap. Quantum dots can fulfill the necessary energy gap requirement by choosing the ones with the right size. It is interesting to note that for the QD to effectively accept the donated electron from the redox mediator. Finally, the maximum potential produced by the cell is determined by the energy separation between the electrolyte chemical potential (E$_{redox}$) and the Fermi level (E$_F$) of the TiO$_2$ layer, as shown in Figure 2.

3. Quantum Dots Energy States and Confinement Effect

Quantum dots can be treated as zero dimensional bulk solid. The density of states can be represented in this case by a delta function, as illustrated in Figure (3-a). In this system only discrete energy levels are allowed with a specific wave vector **k** value for each allowed energy state (Fig. 3-b, 3-c). In the solar spectrum, a high energy photon can produce multiple electron-hole pairs. In this process an energetic photon can excite an electron in the valence band producing an electron-hole pair. The excited electron may produce additional electron-hole pairs by impact ionization [32].

The energy gap of a QD can be estimated as the sum of the band gap energy, the confinement energy, and the bound exciton energy. The band gap energy is determined by the size of the quantum dot. In strong confinement regime, the size of the QD is smaller than the exciton Bohr radius a_{EBR}, where the energy levels split up. In this case we have,

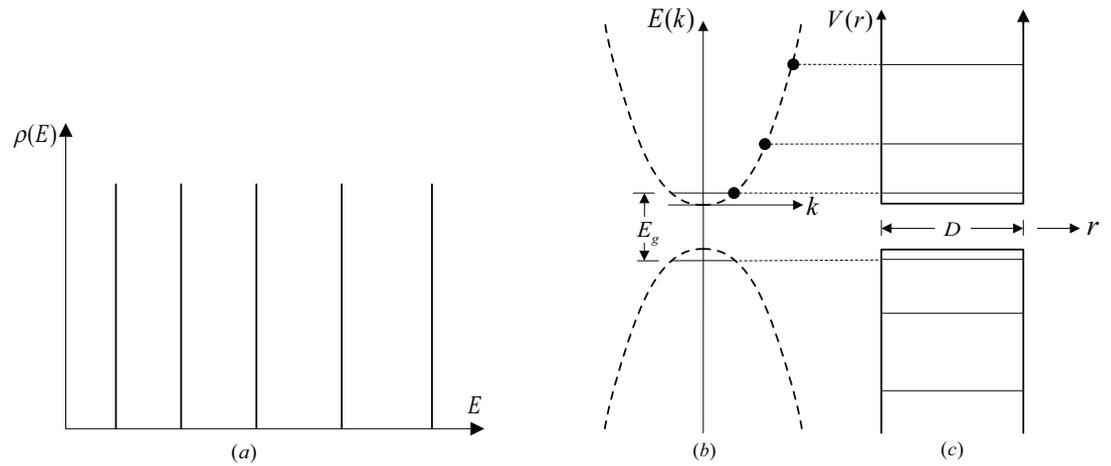$$a_{EBR} = \varepsilon_r \left(\frac{m}{\mu} \right) a_B \qquad (7)$$

Figure 3: a) Energy density of states in QDs is represented by delta functions. b) Due to confinement effect the energy gap is larger than that of the bulk material. c) Allowed energy in QD are ideally those of an infinite quantum well.

where m is the mass, μ is the reduced mass, ε_r is the size dependent dielectric constant, ϵ_0 is the permittivity of free space, and a_B is the Bohr radius. The total energy released in the emission can thus be written as,

$$E_{\text{total}} = E_{\text{bandgap}} + E_{\text{Confinement}} + E_{\text{Exciton}} \tag{8}$$

Where

Hence, according to [18], the last two terms in Eq. (8) are,

$$E_{\text{Confinement}} = \frac{\hbar^2 \pi^2}{2a^2} \left(\frac{1}{m_n} + \frac{1}{m_p} \right) = \frac{\hbar^2 \pi^2}{2\mu \, a^2} \tag{9}$$

and

$$E_{\text{exciton}} = -\frac{1.8 \, e^2}{2\pi\varepsilon\varepsilon_o a} \tag{10}$$

In the above equations m_n and m_p are the electron and hole effective masses respectively, and a is the QD radius. Other quantities are as defined above.

The above simple model shows that the energy of QDs is dominated by the quantum confinement effect (Eq. 9), where the energy varies inversely with the square of the QDs radius.

4. Experimental

Several methods have been employed to prepare TiO_2 layers. We prepared nanostructured layer following the procedure detailed in [5, 6, 9]. In this method, a suspension of TiO_2 is prepared by adding 9 ml of nitric acid solution of PH 3-4 (in ml increment) to 6

g of colloidal P25 TiO_2 powder in mortar and pestle. To get a white free flow-paste, we added 8 ml of distilled water (in 1 ml increment) during the grinding process. Finally, a drop of transparent surfactant is added in 1 ml of distilled water to ensure uniform coating and adhesion to the transparent conducting electrode.

Doctor blade technique was employed by depositing the TiO_2 suspension uniformly on a cleaned (rinsed with ethanol) electrode plate. The TiO_2 layer was allowed to dry for few minutes and then annealed at approximately 450°C (in a well ventilated zone) for about 15 minutes to form a porous large surface area TiO_2 layer. The layer is then allowed to cool slowly to room temperature. This is a necessary condition to remove stresses and avoid cracking of the glass or peeling off the TiO_2 layer. Investigation of the formation of nanoporous TiO_2 layer was confirmed by scanning electron microscopy (SEM) and X-ray diffraction measurements. Once the TiO_2 nanocrystalline layer is prepared, it is coated with PbS QDs suspended in toluene. The counter electrode is coated with graphite that acts as a catalyst in redoxing the excited quantum dots. Both the photo- and the counter electrode are clamped together and drops of electrolyte are applied to fill the clamped cell. The electrolyte used is iodide electrolyte (0.5 M potassium iodide mixed with 0.05 M iodine in water free ethylene glycol) containing a redox couple (traditionally the iodide/tri-iodide I^-/I_3^- couple). The measurements of the open circuit voltage and short circuit current have been performed using home-made solar simulator. A glass sheet has been placed above the cell in order to eliminate or prevent overheating effect. No antireflection coatings on the photoelectrode have been used.

5. Results and Discussion

5.1. Nanocrystalline structure of TiO_2 thin film

Optical measurements demonstrate the effectiveness of sensitizing TiO_2 nanocrystalline layers using different sizes of lead sulfide QDs. The TiO_2 layers were first annealed, and their nanostructure properties were then examined by scanning electron microscope (SEM) measurements. Figure (4) shows the nanocrystalline morphology of the TiO_2 thin film after sintering. Figure (5) shows the X-ray diffraction measurement conducted on our samples. It confirms the formation of nanocrystalline particles with sizes less than 50 nm [9].
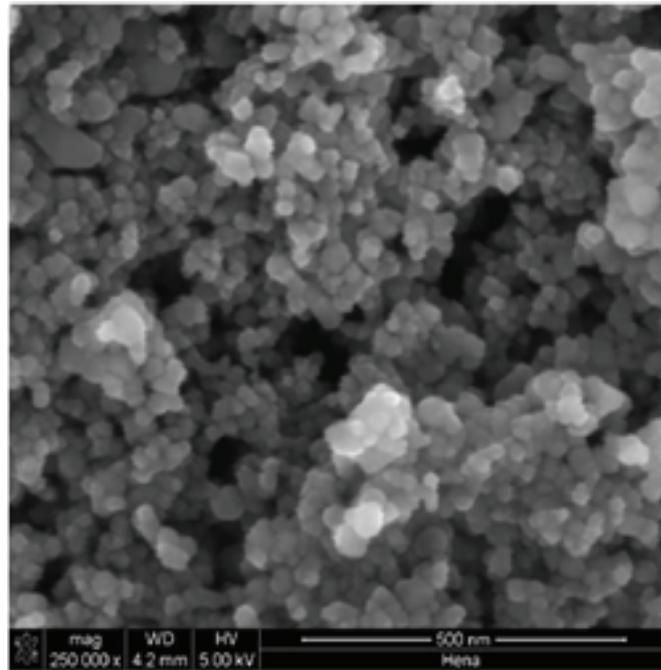
Figure 4: SEM image of nanocrystalline TiO$_2$ annealed at a temperature of 550°C.
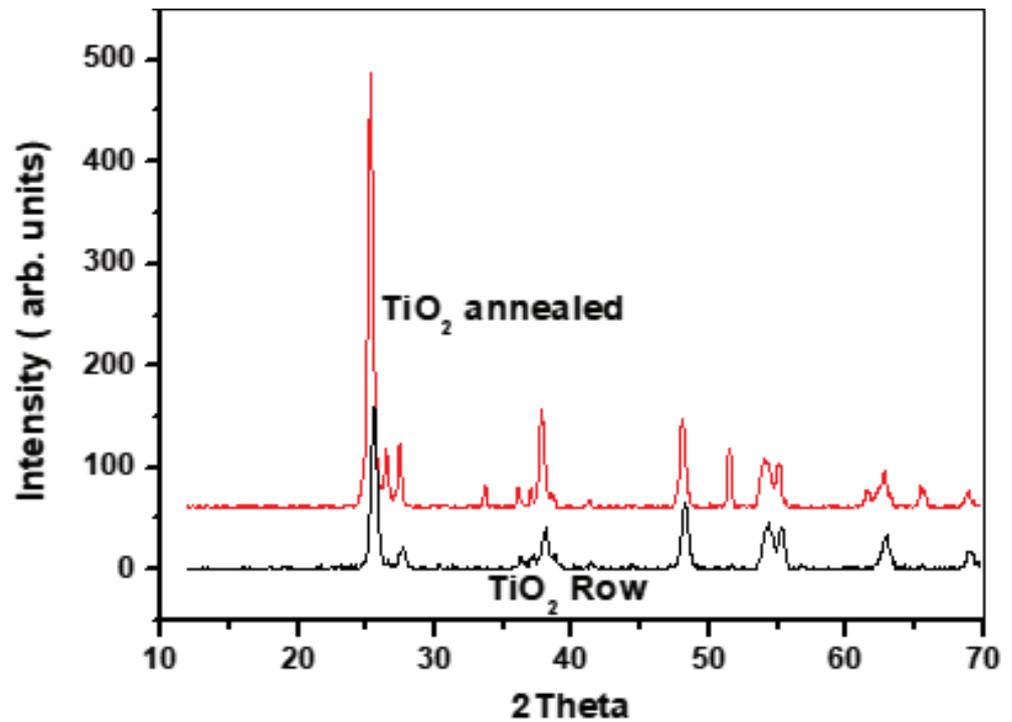

Figure 5: X-ray diffraction measurements of TiO$_2$ layer before and after annealing.

5.2. Absorbance spectra of quantum dots

Figure (6) shows the absorbance of three different sizes of PbS QDs suspended in toluene as a function of wavelength. The measurements were performed using dual

beam UV-VIS spectrophotometer (Shimadzu, model UV-3101). The spectrum is characterized by discrete absorption peaks indicative of the quantum confinement effect. As the size of the QDs increases, the absorbance shifts to longer wavelength. These measurements ensure the effectiveness of PbS QDs as a possible sensitizer. It is to be noted that PbS QDs of 3.2 nm radius are the most appropriate absorber in the visible as well as the near infrared region of spectrum. This feature is of great importance in choosing the most effective sensitizers in our photovoltaic cell.
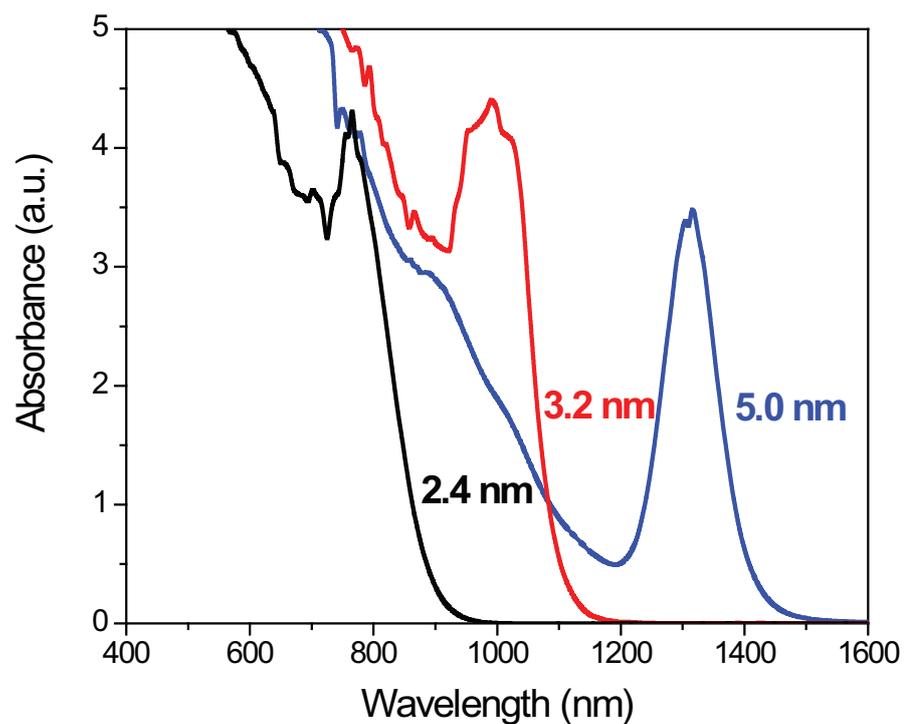

Figure 6: Wavelength dependence of the absorbance of PbS QDs for three different sizes.

5.3. Current injection in TiO$_2$ thin film

Quantum dots adhering directly to the TiO$_2$ layer and are exposed directly to applied illumination could deliver readily an electron from the excited state to the conduction band of the TiO$_2$ layer after surmounting a certain potential barrier at the interface. Two possible mechanisms of current injection are reported [33, 34]. The first is tunneling of electrons across the energy barrier, and the second is the Poole-Frenkel effect resulting from the enhancement of thermal activation due to reduced barrier height under the field [35]. The effectiveness of these processes is determined by the height

of the barrier formed between QDs (depending on their energy gap) and the TiO_2 nanostructured layer.

For non-uniform distribution of QDs we expect having groups of these accumulated in patches where only certain of them are exposed directly to applied illumination. Once a QD of this group is excited, an electron could tunnel to adjacent QD or could follow a non-radiative path and finally lost to the system. Figure (1) shows a schematic representation of QDs distribution on the TiO_2 nanocrystalline film.

5.4. Effect of counter electrode coating on the I - V characteristics

Figure (7) shows the applied voltage-photocurrent characteristics of quantum dot sensitized photovoltaic cell (QDSPC) at room temperature. The cell was fabricated using non-annealed TiO_2 layer as well as without carbon coating of the counter electrode. For non-coated counter electrode the open circuit voltage remains relatively high whereas the short circuit current is dramatically quenched. The open-circuit voltage for cell with 5 nm size PbS QDs is about 273 mV, whereas the short circuit current reaches approximately 10.2 μA. Drastic improvement of the I-V characteristics is obtained for carbon coating of the counter electrode, as demonstrated in the next section.

5.5. Enhanced I-V characteristics of QDs synthesized solar cell

Figure (8) depicts the I-V characteristics of PbS QDs of different sizes. The photocurrent is maximum for a given intermediate size of the QDs. In our case the best result was obtained for 3.2 nm QDs. This behavior seems surprising at first sight, but could be easily explained once a thorough investigation of the spectral response of various elements constituting the cell is considered. This result will be further discussed in the next section. For quantum dots of mixed sizes the photocurrent drops by a factor of 3.5 and the open circuit voltage by a factor of 1.3 with respect to the 3.2 nm radius QD based cell, as illustrated in Figure (8).

5.6. Efficiency of PbS QDs sensitized solar cell

There are three important parameters that characterize the performance of a solar cell. These are the open-circuit voltage (V_{oc}), the short circuit current (I_{sc}), and the fill factor (*FF*). However, the fill factor is also a function of V_{oc} and I_{sc}. Therefore, these last two parameters are the key factors for determining the cell's efficiency.
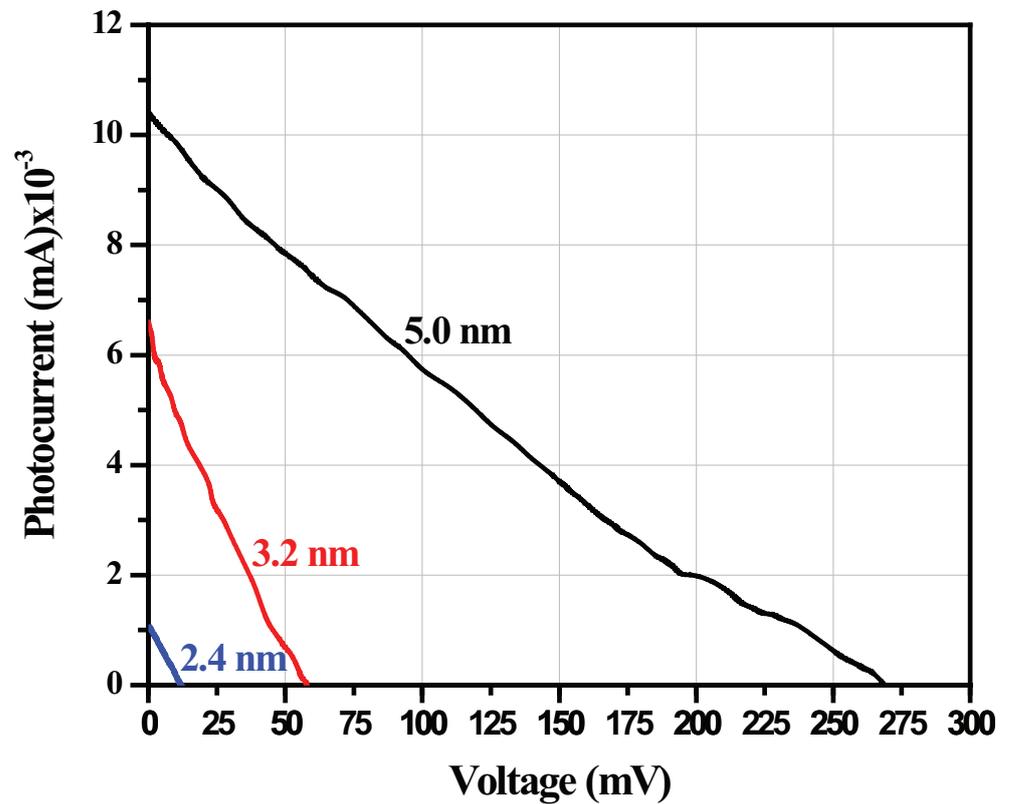
Figure 7: I-V characteristic of QD synthesized solar cells without carbon coated counter electrode.

Under ideal conditions, each photon incident on the cell with energy greater than the band gap will produce an electron flowing in the external circuit. Upon illumination the I-V characteristics are shifted down by the light generated current I_L. Ideally, the short-circuit current I_{sc} is equal to I_L. In this case, the open circuit voltage is given by

$$V_{OC} = \frac{kT}{q} \ln \left(\frac{I_{sc}}{I_o} + 1 \right) \qquad (11)$$

where I_o is the reverse saturation current, T is the temperature in Kelvin, and k is the Boltzmann constant.

The fill factor is determined from the maximum area of the I-V characteristics under illumination and the short circuit current and open circuit voltage, or

$$FF = \frac{V_{mp} \, I_{mp}}{V_{oc} \, I_{sc}} \qquad (12)$$

where V_{mp} and I_{mp} are the operating point that will maximize the power output. In this case, the energy conversion efficiency is given by

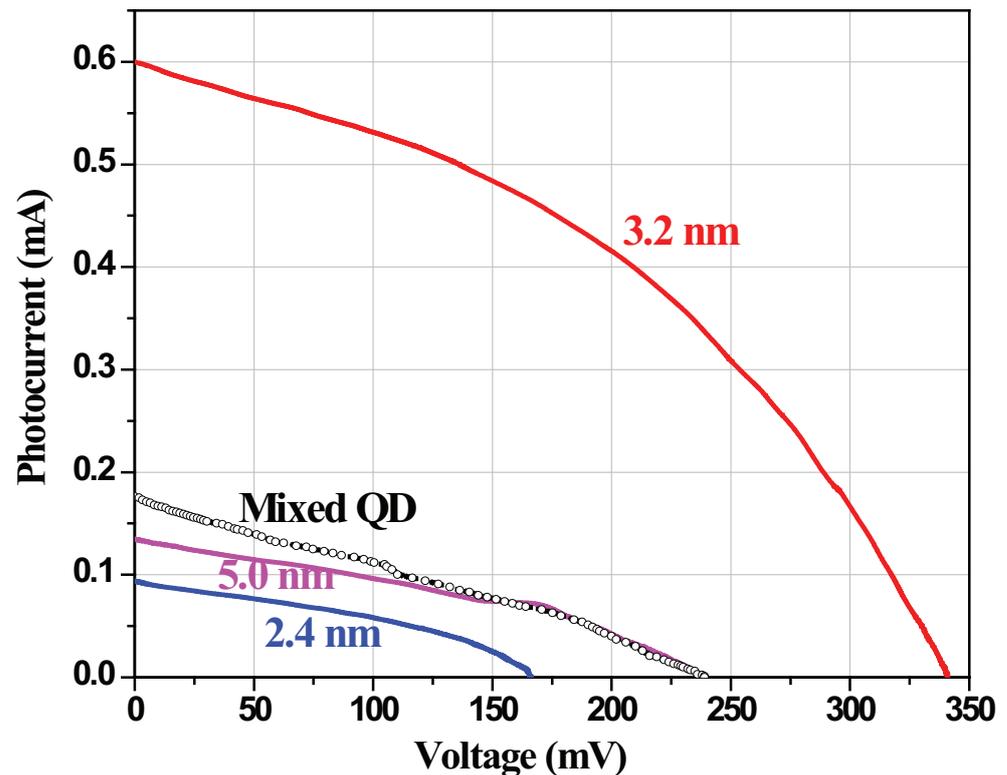$$\eta = \frac{V_{oc} \, I_{sc} \, FF}{P_{in}} \qquad (13)$$

Figure 8: I-V characteristics of PbS QDs solar cells of different sizes and of mixed combinations.

where P_{in} is the input power. Table 1 depicts the short circuit current, the open circuit voltage, the fill factor, and the efficiency for cells of different sizes quantum dots. As the size of the QD is reduced, the open circuit voltage, the photocurrent, the fill factor, and consequently, the efficiency of the cell is reduced. For non-annealed cell, the efficiency is reduced by about three orders of magnitude, the open circuit voltage by a factor of 15, and the short circuit current by a factor of 63. This implies the importance of annealing to optimize the structural requirement for achieving high current injection efficiency. The best power efficiency of 4.47% was obtained for the 3.2 nm radius QDs. For this particular size the effectiveness of current injection is the most promising. Cells based on QDs of mixed sizes have the lowest efficiency. Reported efficiencies in recent published work using either depleted heterojunction colloidal QD solar cells [36] or improved lead sulphide QD solar cell using n-type transition metal oxide [37] give comparable values. It seems unlikely that the effectiveness of injection mechanisms drops suddenly when the sizes of the quantum dots changes slightly. To trace the origin of this behavior we refer first to the absorption spectra (Figure 6). The 3.2 nm QDs have their absorption spectrum centered at about 1000 nm. At this wavelength

the absorption of the 2.4 nm is almost negligible, whereas that of the 5 nm QDs is only slightly enhanced. On the other hand, the absorption spectrum of the glass used as a window assumes its maximum transmittance at about 1000 nm. Therefore, it is highly probable that the reduced efficiencies of cells based on the 2.4 and 5 nm radius QDs are severely influenced by the glass spectral window. A more effective cell design must involve the use of the entire solar spectrum, or at least a good portion of the visible spectral region. For further improvement of the system, the TiO_2 nanoporous layer could be replaced by less resistive materials that have a greater surface to volume ratio. Carbon nanotubes are good candidates to achieve this task. These matters are under investigation and are the subject of methodic research work in our laboratories.

TABLE 1: Open-circuit voltages, short-circuit currents, fill factors, and efficiencies for various sizes of PbS QDs solar cells, and of QDs of mixed radii combinations.

Solar Cell	V_{oc} (mV)	I_{sc} (mA)	V_{mp} (mV)	I_{mp} (mA)	FF(%)	Effe%
5.0 nm	238	0.135	170.3	0.071	37.63	0.65
3.2 nm	341	0.6	211	0.397	40.94	4.47
2.4 nm	166.3	0.093	106.7	0.055	37.94	0.32
Mixed QDs non-annealed TiO_2	19.6	0.00228	9.7	0.00123	26.70	6.37×10^{-4}
Mixed QDs annealed TiO_2	239	0.176	147.8	0.078	27.41	0.615

6. Conclusion

In this work we have studied the performance of PbS QDs synthesized nanocrystalline solar cells. Towards this end, we characterize the structural, electronic, and optical properties of the cells. Three different sizes of PbS QDs were used to optimize the cell performance. Electron scanning microscopy and electron diffraction spectroscopy confirm the formation of nanostructural TiO_2 nanoparticles with sizes less than 50 nm. A model was developed to explain the generation cycle of photocarriers. Absorption measurements are characterized by discrete absorption peaks indicative of quantum confinement effect. In addition, a shift of the absorbance spectra to larger wavelengths with increasing the size of the quantum dots was observed. The current injection mechanisms in terms of tunneling and thermal activation were discussed. It was found that the absence of counter electron coating with graphite is a determining factor for obtaining reasonable I-V characteristics. The open circuit voltage, the short circuit current, the fill factor, and efficiency of different quantum dots sizes as well as for a combination of these were measured. An efficiency of 4.47% was obtained for the

3.2 nm size (radius) QDs, whereas a severe quenching of all cell parameters for other quantum dot sizes was observed. A careful analysis reveals that the transmittance of the cell's glass window is probably at the origin of this effect.

Acknowledgments

References

[1] B. O'Regan, and M. Grätzel, "A Low-cost High-Efficiency Solar Cell Based on Dye-Sensitized Colloidal TiO$_2$ Films". Nature, **353**, 737-740, 1991.

[2] D.E. Carlson and C.R. Wronski, "Amorphous Silicon Solar Cells", Appl. Phys. Lett. **28** p. 671-673, 1976.

[3] Y. Hamakawa, H. Okamoto, Y. Nitta, "Thin Film Silicon Solar Cell", Appl. Phys. Lett. **35** (2), P.187-189, 1979.

[4] K. Yamamoto, M. Yoshimi, Y. Tawada, Y.Okamoto, and Nakajama, "Thin Film Si Solar Cell Fabricated at low Temperature", J.Non Cryst. Solids, **266-269,** 1082-1087, 2000.

[5] Khalil Ebrahim Jasim, "Dye Sensitized Solar Cells-Working Principles, Challenges and Opportunities," In: Solar Cells- Dye-Sensitized Devices, Leonid A. Kosyachenko, (Ed), Chapter 8, pp. 171-204, Book Published by InTech Open Access Publisher, ISBN 978-953-307-735-2, October 2011.

[6] K., Hara and H., Arakawa (2003) *Handbook of Photovoltaic Science and Engineering*, by A. Luque and S. Hegedus (Eds.), Chapter 15, p.663, John Wiley & Sons, Ltd., ISBN: 0-471-49196-9.

[7] B. O' Regan, and M. Gratzel," A low cost, high-efficiency solar cell based on dyesensitized colloidal TiO2 films". *Nature (London, United Kingdom)* vol. 353, pp. 737-740, 1991.

[8] Y. Amao, and T. Komori, "Bio-photovoltaic conversion device using chlorine-e$_6$ derived from chlorophyll from *Spirulina* adsorbed on a nanocrystalline TiO2 film electrode". *Biosensors Bioelectronics*, Vol. 19, pp. 843-847, 2004.

[9] Khalil Ebrahim Jasim, Shawqi Al-Dallal, and Awatef M. Hassan, "Henna (Lawsonia inermis L.) Dye-Sensitized Nanocrystalline Titania Solar Cell," Journal of Nanotechnology, vol. 2012, Article ID 167128, 6 pages, 2012. doi:10.1155/2012/167128. (2012).

[10] Khalil Ebrahim Jasim, "*Natural Dye-Sensitized Solar Cell Based On Nanocrystalline TiO₂,"* Sains Malaysiana, vol 41(8), pp. 1011-1016. (2012).

[11] H. Gerischer and H. Tributsch, "*Electrochemische Untersuchungen zur spectraleu sensibilisierung von ZnO-Einkristallen",* ber. Bunsen. Ges. Phys. Chem, **72**, 437- 445, 1968.

[12] H. Gerischer and H. Tributsch, The use of semiconductor electrodes in the study of photochemical reactions. ber. Bunsen. Ges. Phys. Chem, **72**, 251- 260, 1969.

[13] Chiba, Y.; Islam, A.; Watanabe, Y; Komiya, R.; Koide, N.; Han, L., "Dye-sensitized solar 29 cells with conversion efficiency of 11.1%. Japanese Journal of Applied Physics, Part 2:30 Letters & Express Letters", Vol. 45, pp. 24-28, 2006.

[14] M. Law, L. E. Greene, J. C. Johnson, R. Saykally, and P. D. Yang, "Nanowire dye sensitized solar cells". Nature Materials, Vol. 4, 455-459, 2005.

[15] G.P. Smestad, "Education and solar conversion: Demonstrating electron transfer, Sol. Energy Mater". Sol. Cells, Vol. 55, pp. 157-178, 1998.

[16] A. P. Alivisatos, "Semiconductor clusters, Nanocrystals, and Quantum Dots" Science, New Series, Vol. 271, No. 5251, pp. 933-937, 1996.

[17] S. M., Reimann and M. Manninen, C, "Electronic structure of quantum dots" Reviews of Modern Physics, Vol. 74, pp. 1283-1342, 2002.

[18] L. E. Brus, "Electronic Wavefunctions in Semiconductor Clusters," Feature Article, J. Phys. Chem., Vol. 90, pp. 2555, 1986.

[19] R. J. Ellingson, M. C. Beard, J. C. Johnson, P. Yu, O. I Micic, A. J. Nozik, A. Shabaev, A. L. Efros, " Highly Efficient Multiple Exciton Generation in Colloidal PbSe and PbS Quantum Dots". Nano Lett. 5, 865–871, 2005.

[20] R. D. Schaller, and V. I. Klimov, "High Efficiency Carrier Multiplication in PbSe Nanocrystals: Implications for Solar Energy Conversion". Phys. Rev. Lett. 92, 186601, 2004.

[21] Khalil Ebrahim Jasim, and Awatef M. Hassan "Nanocrystalline TiO₂ Based Dye Sensitized Solar Cells" International Journal of Nanomanufacturing. Vol. 4, Nos. 1/2/3/4, pp. 242-247, (2009).

[22] Khalil Ebrahim Jasim, Shawqi Al-Dallal, and Awatef M. Hassan, "Natural dye-sensitised photovoltaic cell based on nanoporous TiO₂" Int. J. Nanoparticles, Vol. 4, No. 4 (2011).

[23] H. J. Lee, J. H. Yum, H. C. Leventis et al., "CdSe quantum dot-sensitized solar cells exceeding efficiency 1% at full-sun intensity," Journal of Physical Chemistry C, vol. 112, no. 30, pp. 11600–11608, 2008.

[24] J. H. Bang and P. V. Kamat, "Quantum dot sensitized solar cells. A tale of two semiconductor nanocrystals: CdSe and CdTe," *ACS Nano*, Vol. 3, no. 6, pp. 1467–1476, 2009.

[25] A. Peng and X. Peng, "Formation of high-quality CdTe, CdSe, and CdS nanocrystals using CdO as precursor". Journal of the American Chemical Society, vol. 123, no. 1, pp. 183–184, 2001.

[26] P. Wang, S. M. Zakeeruddin, J.E. Moser, M. K. Nazeeruddin, T.Sekiguchi, M. Grätzel, "Molecular-scale interface engineering of TiO_2 nanocrystals: Improving the efficiency and stability of dye-sensitized solar cells". Nat. Mater. **2**, 402, 2003.

[27] P. Wang, S. M. Zakeeruddin, P./Comte, I. Exnar, and M. Grätzel. "Gelation of Ionic Liquid-Based Electrolytes with Silica Nanoparticles for Quasi-Solid-State Dye-Sensitized Solar Cells". Chem. Commun., 2972-2973, 2002.

[28] J. Gao, C.L. Perkins, J. M. Luther, M. C. Hanna, H. Chen, O. E. Semonin, A. J. Nozik, R.J. Ellingson, and M.C. Beard, "n-Type transition metal oxide as hole extraction layer in PbS quantum dot solar cells" Nano Letter., Vol. 11, pp.3263, 2011.

[29] A. Braga, S. Gimenez, I. Concina, A. Vomiero, and I. Mora-Sero, "Panchromatic sensities solar cells based on metal sulfied quantum dots grown directly on nanostructured TiO_2 electrodes" J.Phys. Chem. Lett., Vol.2, pp. 454-460, 2011.

[30] X. W, G.I. Koleilat, J. Tang, H. Liu, I.J. Kramer, R. Debnath, L. Brzozowski, D.A. R. Barhouse, L. Levina, and S. Hoogland, "Tandem colloidal quantum dot solar cells employing a graded recombination layer" nature photon., published online 26 June 2011.

[31] I. Hod, V. Gonzalez-Pedro, Z. Tachan, F. Fabregat-Santiag I. Mora-Sero, J. Bisquert, and A. Zaban, "Dye versus Quantum Dots in Sensitized Solar Cells: Participation of Quantum Dot Absorber in the Recombination Process", J. Phys. Chem. Lett., 2, 3032–3035, 2011.

[32] J. Nozik,"Multiple exciton generation in semiconductor quantum dots." Chemical Physics Letters, Vol. 457, pp. 3-11, 2008.

[33] E. S. Shatalina, S. A. Blokhin, A. M. Nadtochiy, A. S. Payusova, A. V. Saveliev, M. V. Maximov, A. E. Zhukov, N. N. Ledentsov, A. R. Kovsh, S. S. Mikhrin, and V. M. Ustinov, "Analysis of mechanisms of carrier emission in the p-i-n structure with In (Ga) ad quantum dot" semiconductors, **44**, 1308, 2010.

[34] W. H. Chang, T. M. Hsu, C. C. Huang, S. L. Hsu, C. Y. Lai, N. T. Yeh, and J.-I. Chyi, Phys. Rev. B **62**, 6959, 2000.

[35] J. L. Hartke, The Three−Dimensional Poole−Frenkel Effect, J. Appl. Phys., **39**, 4871, 1968.

[36] A. G. Pattantyus-Abraham et al. "Depleted-heterojunction colloidal quantum dot solar cells" ACS Nano **4**, 3374-3380, 2010.

[37] J. Gao, L. C. Perkin, J. M. Luther, M. C. Hanna, Hsiang-Yu Chen, O. E. Semonin, A. J. Nozik, R. J. Ellingson, and M. C. Beard. "n-Type Transition Metal Oxide as a Hole Extraction Layer in PbS Quantum Dot Solar Cells". Nano Letters 11, 3263, 2011.